Journal of Catalysis 270 (2010) 16–25

Contents lists available at ScienceDirect

Journal of Catalysis

journal homepage: www.elsevier.com/locate/jcat

Aerobic oxidation of cyclohexane by gold-based catalysts: New mechanistic insight by thorough product analysis

Bart P.C. Hereijgers, Bert M. Weckhuysen *

Inorganic Chemistry and Catalysis Group, Debye Institute for NanoMaterials Science, Utrecht University, Sorbonnelaan 16, 3508 TB Utrecht, The Netherlands

ARTICLE INFO

Article history:
Received 30 October 2009
Revised 29 November 2009
Accepted 2 December 2009
Available online 29 December 2009

Keywords:
Gold
Selective oxidation
Autoxidation
Cyclohexane
KA-oil
Radical-chain mechanism
Heterogeneous catalysis

ABSTRACT

The selective oxidation of cyclohexane to cyclohexanone and cyclohexanol with air over Au/Al_2O_3, Au/TiO_2, and Au/SBA-15 catalysts was investigated and compared with the industrial autoxidation process. In contradiction with the literature results, the Au-based catalysts did not exhibit excellent catalytic performance and the combined selectivity toward cyclohexanone and cyclohexanol decreased to ~70% with the increasing conversion above 5%. In addition, the observed product evolution and by-product evolution were typical for the autoxidation process, although a significant increase in adipic acid and CO_2 formation was observed. Additional oxidation experiments containing a radical scavenger completely inhibited the reaction and provided proof that the oxidation follows a radical-chain mechanism instead of a catalytic mechanism. This explains the low selectivity at increasing conversion. This important deviation from the literature results can be clarified by the complicated but necessary product analysis of both the gas and the liquid phases.

1. Introduction

The liquid-phase aerobic oxidation of cyclohexane (CyH) is of major importance for the production of cyclohexanone and cyclohexanol (ketone/alcohol or KA-oil), the annual worldwide production of which exceeds 10^6 tons [1,2]. Both oxidation products are the main industrial precursors of, respectively, ε-caprolactam and adipic acid, building blocks of the nylon-6 and nylon-6,6 polymers [1]. Commercially the aerobic oxidation process is operated at temperatures of 415–435 K and 1–1.5 MPa pressure. In industry, the conversion is kept at 4% to prevent the formation of excessive amounts of by-products by over-oxidation of the relatively reactive oxygenates, giving 70–85% selectivity toward KA-oil [1–3]. For the production of ε-caprolactam, the ketone is considered as the most valuable product and consequently a high K/A-ratio is desired.

In essence there are two commercial processes exploited nowadays, i.e., the non-catalytic autoxidation process and the catalyzed process. In the first process, cyclohexyl hydroperoxide (CyOOH) is formed non-catalytically, followed by a subsequent step converting CyOOH catalytically to KA-oil with typical K/A-ratio of 1.5 [4,5]. The second process makes use of a radical initiator, mostly dissolved cobalt(II)naphthenate, to accelerate the process resulting in a K/A-ratio 0.3–0.5 [3,6,7]. Although the product distribution in both processes differs, the autoxidation as well as the catalyzed reaction is known to proceed via the complex radical-chain mechanism shown in reactions (1)–(5) [8]. The chain initiation is considered to proceed through the homolytic cleavage of cyclohexyl hydroperoxide (CyOOH) according to reaction (1). Transition metals capable of undergoing a one-electron switch (e.g., Co^{2+}, Mn^{2+}, and Cr^{2+}) are able to catalyze this initiation via a so-called Haber-Weiss cycle (Scheme 1) [3,9–12]. Once formed, the oxygen-centered radicals can attack the CyH solvent via reaction (2) to form cyclohexyl radicals. Via the rapid reaction (3) with molecular O_2 these radicals will form cyclohexyl peroxy radicals ($CyOO^{\cdot}$). $CyOO^{\cdot}$ is the main chain propagator causing the continuous formation of new radicals as in reactions (3), (4). The formation of cyclohexanol (CyOH) and cyclohexanone (Cy=O) was long time attributed to the chain termination by mutual destruction of two peroxy radicals according to reaction (5) [2,3,8,13]. However, recent research by Hermans et al. provided strong evidence that subsequent propagation reactions of CyOOH within their Franck-Rabinowitch solvent cage are responsible for the formation of both the ketone and the alcohol [14,15].

$$CyOOH \rightarrow CyO^{\cdot} + {}^{\cdot}OH \quad (1)$$

$$CyO^{\cdot} + CyH \rightarrow CyOH + Cy^{\cdot} \quad (2)$$

$$Cy^{\cdot} + O_2 \rightarrow CyOO^{\cdot} \quad (3)$$

$$CyOO^{\cdot} + CyH \rightarrow CyOOH + Cy^{\cdot} \quad (4)$$

$$2CyOO^{\cdot} \rightarrow CyOH + Cy{=}O + O_2 \quad (5)$$

* Corresponding author. Fax: +31 (0) 30 251 1027.
E-mail address: b.m.weckhuysen@uu.nl (B.M. Weckhuysen).

0021-9517/$ - see front matter © 2009 Elsevier Inc. All rights reserved.
doi:10.1016/j.jcat.2009.12.003

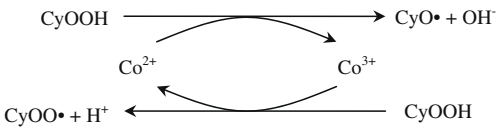

Scheme 1. Haber-Weiss cycle of the cobalt-catalyzed decomposition of cyclohexyl hydroperoxide.

Especially at higher conversion (>5%), excessive by-product formation is observed [6], which has for a long time been attributed to the ring cleavage of cyclohexanone [3]. Recently Hermans et al. proved that the hitherto overlooked propagation of cyclohexyl hydroperoxide CyOOH into a cyclohexoxy radical (CyO·) and subsequent β-cleavage forming a ring-opened ω-formyl radical is the most important origin of by-product formation [11,13]. The nature of these by-products, e.g., peroxides, organic acids, and gasses, complicates the analysis of the reaction mixture tremendously [8]. Performing accurate selectivity calculations and obtaining a complete mass balance are therefore not straightforward and is often underestimated [6].

Since radical chemistry plays the key role in by-product formation in cyclohexane oxidation, one should aim, in order to improve the yield of the desired products, for a non-radical, catalytic conversion of CyOOH to avoid the formation of CyO· intermediates [13]. Triggered by the successes of gold-based catalysts in a wide variety of selective oxidation reactions [16–18], the use of nanostructured gold catalysts for this particular oxidation reaction was initiated by Suo et al. in 2004. Au/ZSM-5 and Au/MCM-41 catalysts were found to be able to convert cyclohexane to KA-oil at 150 °C and 1 MPa oxygen pressure reaching 90+% selectivity at conversion of 10–15% [19,20]. These promising results were confirmed by the publications coming from a variety of groups reporting similar results at similar conditions for, e.g., (modified) Au/Al_2O_3 [21,22] and gold nano-particles supported on amorphous Ti-doped SiO_2 [23] and mesoporous silica materials [24–26]. In combination with *t*-butyl hydroperoxide as initiator, Au/C was found to exhibit a high selectivity toward K/A-oil formation only at low conversion, decreasing significantly when the conversion increased [27,28].

The results published justify a more thorough investigation of the excellent catalytic performances of these supported gold catalyst materials, especially since the product distribution during reaction has received minor attention so far. In this regard, we show in this work that the aforementioned results on gold-based catalysts are obscured by the complicated product analysis. In fact, the gold-based catalysts are relatively inert and the reaction path follows the above-described radical-chain mechanism.

2. Experimental methods

2.1. Catalyst preparation

Supported gold nano-particles were prepared by deposition precipitation on the different supports from a dilute $HAuCl_4$ (Sigma–Aldrich, 99.99%) in HCl solution containing the exact amount of gold to achieve a 1 wt% loading. Precipitation was performed with a diluted ammonia solution (Merck, 25%) at a pH of 9.5 [29]. The support materials were obtained from a commercial source; i.e., γ-Al_2O_3 (Engelhard, S_{BET} = 230 m^2/g, total pore volume = 0.76 cm^3/g) and TiO_2 (Degussa P25, S_{BET} = 55 m^2/g, total pore volume = 0.19 cm^3/g). The SBA-15 support (S_{BET} = 696 m^2/g, total pore volume = 0.797 cm^3/g) was home synthesized following the procedure as described by Zhao et al. [30].

2.2. Catalyst characterization

TEM micrographs were obtained on a FEI Tecnai 20F Transmission electron microscope operated at 200 KeV equipped with a Schottky Field Emission Gun (magnification range is 25×–700k×) and a FEI Tecnai 12 Transmission Electron Microscope operated at 120 KeV (magnification range is 40×–700k×). The gold particle size distributions as determined from TEM represent at least 210 particles per catalyst material. Diffuse reflectance UV–vis-NIR spectra were recorded on a Varian Cary 500 Scan spectrophotometer. X-ray powder diffraction was performed on a Bruker AXS Advance D8 apparatus using $Co_{K\alpha}$ radiation (λ = 1.78897 Å) operating at 45 kV and 30 mV. N_2-physisorption isotherms and specific surface areas were measured on a Micromeretics Tristar 3000 analyzer. Fourier Transform Infrared (FT-IR) spectra were recorded in transmission mode on a Perkin–Elmer System 2000 FT-IR spectrometer using the KBr technique, in the range of 4000–400 cm^{-1} with a resolution of 1 cm^{-1}.

2.3. Cyclohexane oxidation experiments

Prior to conducting oxidation experiments, the reactor interior was passivated by boiling with a saturated sodium pyrophosphate (ABCR, 99%) solution for 4 h and thorough washing. The aerobic catalytic oxidation experiments were carried out in a fed-batch 500 mL stainless steel autoclave reactor setup (SA182-F316, rated up to 254 bar at 450 °C working conditions) by Autoclave Engineers. The oxidation reactions were performed at 150 °C at 1.2–1.5 MPa under continuous flow (900 sccm) of 8 vol% O_2/N_2 in order to operate outside the flammability range of cyclohexane [31,32]. The gas flows were controlled by Brooks mass flow controllers (type 5850i).

Typically 310 mL cyclohexane (241 g, 2.85 mol, Sigma–Aldrich, 99.5%) containing 1 mol% biphenyl (Acros, 99%) as internal standard was loaded in the reactor and the reactor was flushed with nitrogen. The reactor was heated to a stable operation temperature and subsequently O_2 was introduced, defining t = 0. The effluent gas was cooled in a reflux cooler to diminish the evaporation loss of cyclohexane and volatile organics from the reactor. Remaining gas-phase volatiles were collected in a cold trap. The effluent gas stream was analyzed on-line by gas chromatography (GC) using a Varian CP4900 Micro-GC, double channel on-line GC equipped with porabond Q and 5MS molsieve column and TC detectors. To monitor the O_2 conversion and CO/CO_2 formation the N_2 signal was used as internal standard.

Liquid-phase aliquots were extracted from the reactor via a manually operated sample valve equipped with a filter (5 μm) and thermally quenched. Liquid-phase samples were collected after flushing the tubing with approximately 5 mL of the reactor content. Prior to the liquid-phase product analysis, the samples were dissolved in pyridine (Fluka, 99%) and derivatized with an excess N-methyl N-trimethylsilyl trifluoroacetamide (MSTFA, ABCR, 97%). The silylated samples were analyzed using a Varian 430 GC, equipped with a VF-5 ms column (30 m, DF = 0.25 μm, 0.25 mm I.D.), CP-8400 autosampler, and FID detector, in split/splitless injection mode. The injector temperature was set to 220 °C.

The product-specific FID response has been determined with respect to biphenyl for all main products and by-products including cyclohexanol, cyclohexanone, formic acid, acetic acid, butyric acid, valeric acid, caprioc and hydroxy-caproic acid, glutaric acid, and adipic acid as well as methanol, 1-butanol, 1-pentanol, and 1-hexanol. To determine the FID response factor for cyclohexyl hydroperoxide, the reaction samples were double analyzed, before and after reducing CyOOH to cyclohexanol with triphenyl phosphine (Acros, 99%). For the cobalt-catalyzed reaction cobalt–methylhex-

anoate (Sigma–Aldrich, 65 wt% Co^{2+} in mineral spirits) was used. Radical inhibition experiments were performed using hydroquinone (ABCR, 99%) as inhibitor [33,34].

3. Results

3.1. Catalyst characterization

The catalyst materials under study were characterized by diffuse reflectance UV–vis-NIR spectroscopy, TEM, X-ray powder diffraction, and N_2-physisorption. The presence of supported Au nano-particles was confirmed by the distinctive pink/purple color of the catalyst material after calcination. In Fig. 1 the UV–vis-NIR absorption spectra of the catalysts are shown. The typical absorption band around 500–550 nm, caused by the surface plasmon vibration of colloidal gold, is clearly visible [35]. TEM micrographs of the catalyst materials and related particle size distributions, as determined from TEM images are shown in Fig. 2. The gold particles are clearly visible and exhibit an average particle size of 4.7, 4.8, and 4.0 nm for Au/TiO_2, Au/Al_2O_3, and Au/SBA-15, respectively. The determined particle sizes are similar to the particle sizes reported to form active cyclohexane oxidation catalyst materials [21–23,25]. From the TEM micrographs of Au/SBA-15 it appeared that the SBA-15 support was slightly damaged. Most likely this originates from the Au deposition precipitation at pH = 9.5. This was confirmed by an observed decrease in the S_{BET} (553 m^2/g) and total pore volume (0.694 cm^3/g) as determined from N_2-physisorption after Au deposition. Crystallinity of the catalyst materials was verified by XRD. Only in the case of the Au/SBA-15 catalyst, diffraction lines of gold particles could be observed at 2θ values of 44.8° and 52°. The XRD patterns of Au/Al_2O_3 and Au/TiO_2 showed the broad diffraction lines characteristic for γ-Al_2O_3 and the TiO_2 rutile and anatase phases [36].

3.2. Catalytic testing

To evaluate the inertness of the reactor interior (the stainless steel vessel wall, impellor, thermo-well, cooling coil, and filtered diptube) first of all blank oxidation experiments without catalyst material were conducted. The results are displayed in Fig. 3. It is observed that the autoxidation in the untreated reactor goes through an initiation period of 40 min in which almost no conversion is observed (0.16 mol%). Thereafter, the conversion increased gradually to reach 4% after 104 min on stream. After passivation of the reactor it is clearly observed that the initiation time of the oxidation reaction is extended to 60 min [37]. A conversion of 0.19 mol% was obtained after 60 min of reaction after which the reaction rate increased. Four percent conversion was reached only after 184 min of reaction. It is obvious that, although the reactor is not to be considered "inert", the contribution of the reactor after passivation to the oxidation rate is considerably low. Comparing this to the gold-catalyzed reaction, it is clearly visible that the reaction still exhibited an initiation period (30–45 min) but proceeded significantly faster compared to the uncatalyzed reaction in the passivated reactor. Therefore, we can truly address the activity of the supported gold nano-particles in further experiments.

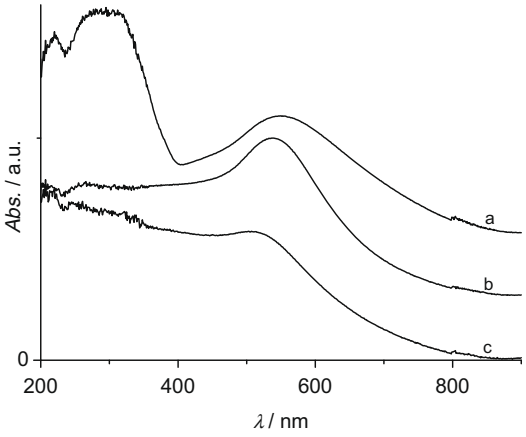

Fig. 1. Diffuse reflectance UV–vis-NIR spectra of (a) Au/TiO_2, (b) Au/Al_2O_3, and (c) Au/SBA-15.

The product distribution and outlet oxygen concentration with the conversion for cyclohexane autoxidation are presented in Fig. 4. The results obtained on the Co^{2+}-catalyzed reaction are included as well for direct comparison with the industrial process. Some reaction characteristics at the industrially applied conversion of 4% cyclohexane are listed in Table 1 for comparison. For all oxidation experiments during the initiation period a buildup of CyOOH is observed, followed by a gradual loss in CyOOH selectivity, caused by conversion into mainly CyOH and Cy=O. With increasing conversion, selectivity toward Cy=O increased for all experiments, however, the obtained K/A-ratios at 4% conversion range from 0.43 (Co^{2+}) to 1.23 (untreated reactor). When the conversion is increased further above 5% the combined selectivity toward KA-oil and CyOOH dropped significantly due to the formation of by-products. In all cases the selectivity toward 6-hydroxy-caproic acid is observed to increase and level off or even decrease subsequently. Adipic acid formation was in general lower in the first period, but increased at higher conversion. Also significant CO and CO_2 formation is observed. The C_6 group (defined as the unidentified species with a retention time longer than caproic acid, so mostly C_6-poly-oxygenates), accounted for 5–10% of the products at 4% conversion, although at higher conversion this increased to 10–20%. The formation of shorter acids (which generally form under oxygen starvation) was low indicating that the reaction was not significantly limited by the oxygen supply [13].

The product selectivity evolution versus CyH conversion for the Au-catalyzed oxidation reactions are presented in Fig. 5. When comparing these to the autoxidation results presented in Fig. 4 some differences are observed. However, in general, the oxidation seemed to follow the same route leading to the same products and by-products. One significant difference is that the S_{CyOOH} at conversions >2% was lower than that was observed for the cobalt-catalyzed oxidation and autoxidation. This lower selectivity coincided with the formation of Cy=O and CyOH immediately from the start of the reaction. At low conversion (<2%) a minimum in $S_{Cy=O}$ was observed. One other remarkable is that, when employing a gold-based catalyst CO_2 formation was observed at lower conversion than CO formation was observed and moreover, CO_2 formation was preferred over CO formation. This is contrary to observations during the autoxidation as well as the cobalt-catalyzed oxidation. The selectivities toward the other main by-products, 6-hydroxy-caproic acid and adipic acid, are comparable through all experiments, although the gold-based catalysts exhibited a relative high adipic acid formation as compared to 6-hydroxy-caproic acid. In total, over 40 different products were found in the final reaction mixture. Reduction of liquid-phase samples with triphenyl phosphine revealed the presence of different peroxide species, e.g., 6-hydroperoxo-caproic acid [38]. The presence of organic acids was confirmed by the extraction of the final oxidation mixture with NaOH (aq) prior to GC analysis.

Interestingly, combining a gold-based catalyst with 1.5 ppm dissolved Co^{2+} led to a performance more or less being the average of the cobalt and the gold-catalyzed process. This is illustrated in Fig. 5d for Au/SBA-15 combined with 1.5 ppm Co^{2+}. The initiation of the reaction was faster, reducing the time to reach 4% conversion

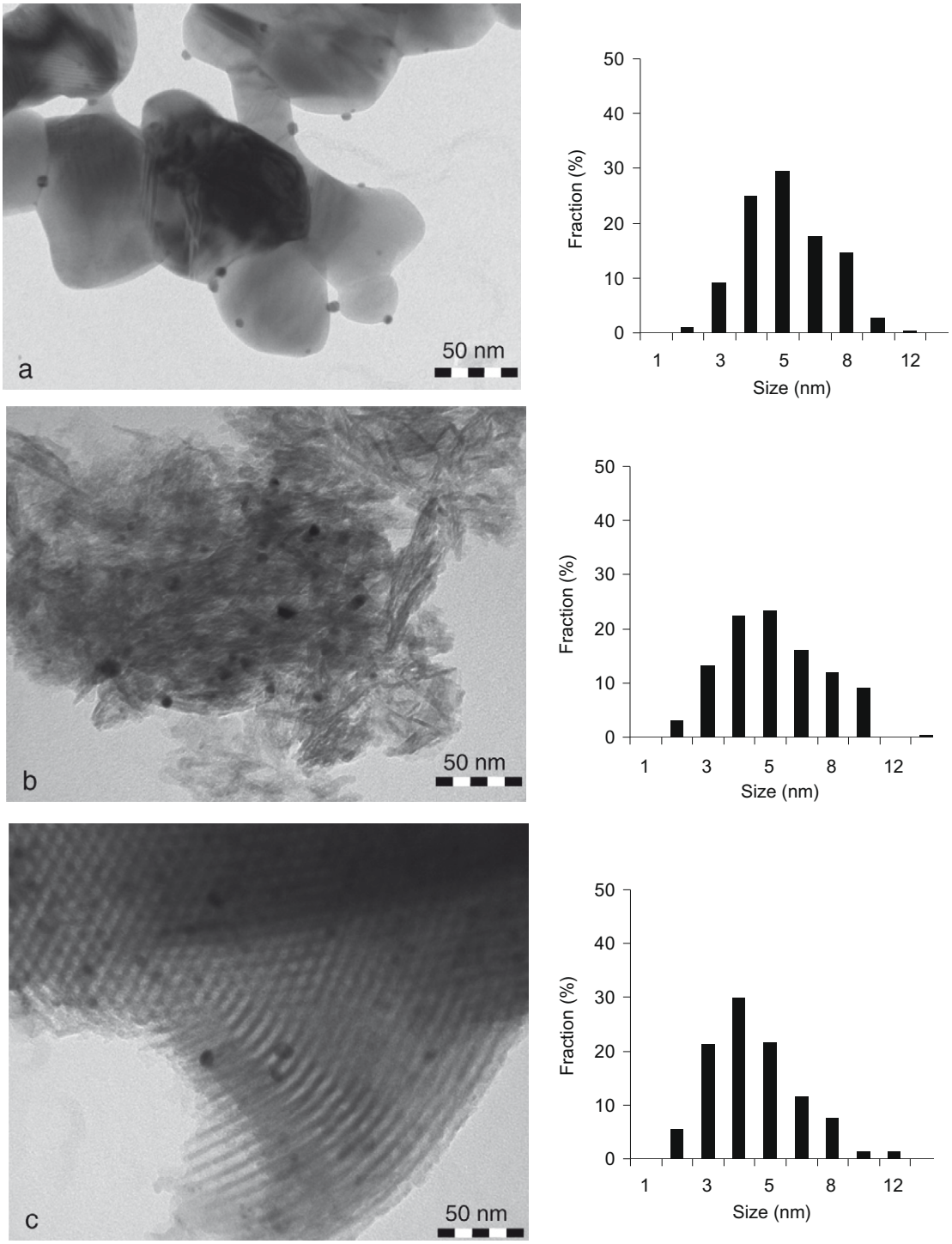

Fig. 2. TEM micrographs and particle size distributions of Au/TiO_2 (a), Au/Al_2O_3 (b), and Au/SBA-15 (c). Particle size distributions represent at least 210 particles.

from 92 to 73 min. However, the observed rate was lower than that when solely 1.5 ppm Co^{2+} was used. Remarkably, the product distribution mimicked the gold-based catalyst results instead of the results obtained with dissolved cobalt salt. Whereas the cobalt-catalyzed reaction first shows a buildup of CyOOH ($S_{CyOOH,initial}$ = 60%), in combination with a Au/SBA-15 catalyst a much lower S_{CyOOH} (35%) was observed favoring the initial formation of CyOH (37%) and Cy=O (24%). Additionally, a relative high adipic acid: hydroxy-caproic selectivity ratio and significant CO_2 formation were observed. Both were shown to be typical for the gold-catalyzed reaction (*vide supra*). This suggests that the oxidation product and by-product formation is dominated by the less efficient initiator, namely gold.

The evolution of the $S_{K/A}$ and the K/A-ratio with increasing conversion for the different cyclohexane oxidation reactions is presented in Fig. 6. For all gold-based catalysts under investigation the evolution of $S_{K/A}$ with increasing conversion followed the same trend as is observed in the autoxidation reaction. The combined selectivity toward the products dropped below 80% already at 3.5% conversion and decreased gradually with increasing

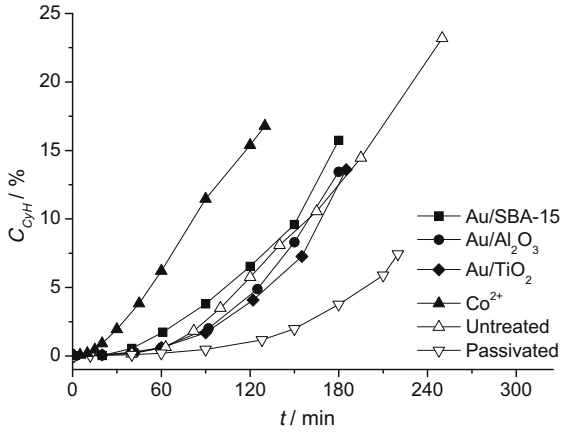

Fig. 3. Conversion versus time on stream during cyclohexane autoxidation (open symbols) and catalyzed oxidation (solid symbols) at 150 °C and 1.2–1.5 MPa.

conversion. Comparing this to the cobalt-catalyzed oxidation it is clearly visible that the $S_{K/A}$ is more favorable in the latter case since a stable selectivity of ~80% is maintained when the CyH conversion increases from 5% to 10%. In terms of K/A-ratio, the autoxidation in the untreated reactor exhibited the best performance, yielding a K/A-ratio increasing of 1.23 at 4% conversion.

Table 1
Cyclohexane oxidation results for gold-based catalysts at 423 K and 1.2–1.5 MPa referenced to the autoxidation and the cobalt-catalyzed oxidation reaction. $t_{4\%}$ = time passed until 4% conversion was reached. Selectivities and K/A-ratio are determined at 4% conversion. For the cobalt-catalyzed oxidation reaction 1.5 ppm Co^{2+} was used.

Catalyst	$t_{4\%}$ (min)	Selectivity (%)			K/A-ratio
		K	A	CyOOH	
Untreated reactor	104	43	35	11	1.23
passivated reactor	184	21	28	29	0.75
Co^{2+}	46	17	48	17	0.35
Au/SBA-15	92	28	43	7	0.65
Au/Al_2O_3	115	18	42	19	0.43
Au/TiO_2	121	20	45	15	0.44
Au/SBA-15 and Co^{2+}	73	23	52	8	0.44
Au/TiO_2 and Co^{2+}	77	20	47	15	0.43

This was most probably caused by chromium present in the stainless steel reactor surface which is known to catalyze the dehydration of CyOOH into Cy=O [3,12,39]. Passivation of the reactor resulted in a lower obtained K/A-ratio (<1) typical for autoxidation [13,37,40]. In the cases of the catalyzed reactions, lower K/A-ratios were observed, i.e., 0.34 and 0.65 for Co^{2+} and Au/SBA-15, respectively. Note that the value of 0.34 for the cobalt-catalyzed reaction is in good agreement with the literature values for CyOOH decomposition in the presence of cobalt salts, e.g., 0.45 for cobalt(II)methyl-hexanoate [3,7]. The influence of

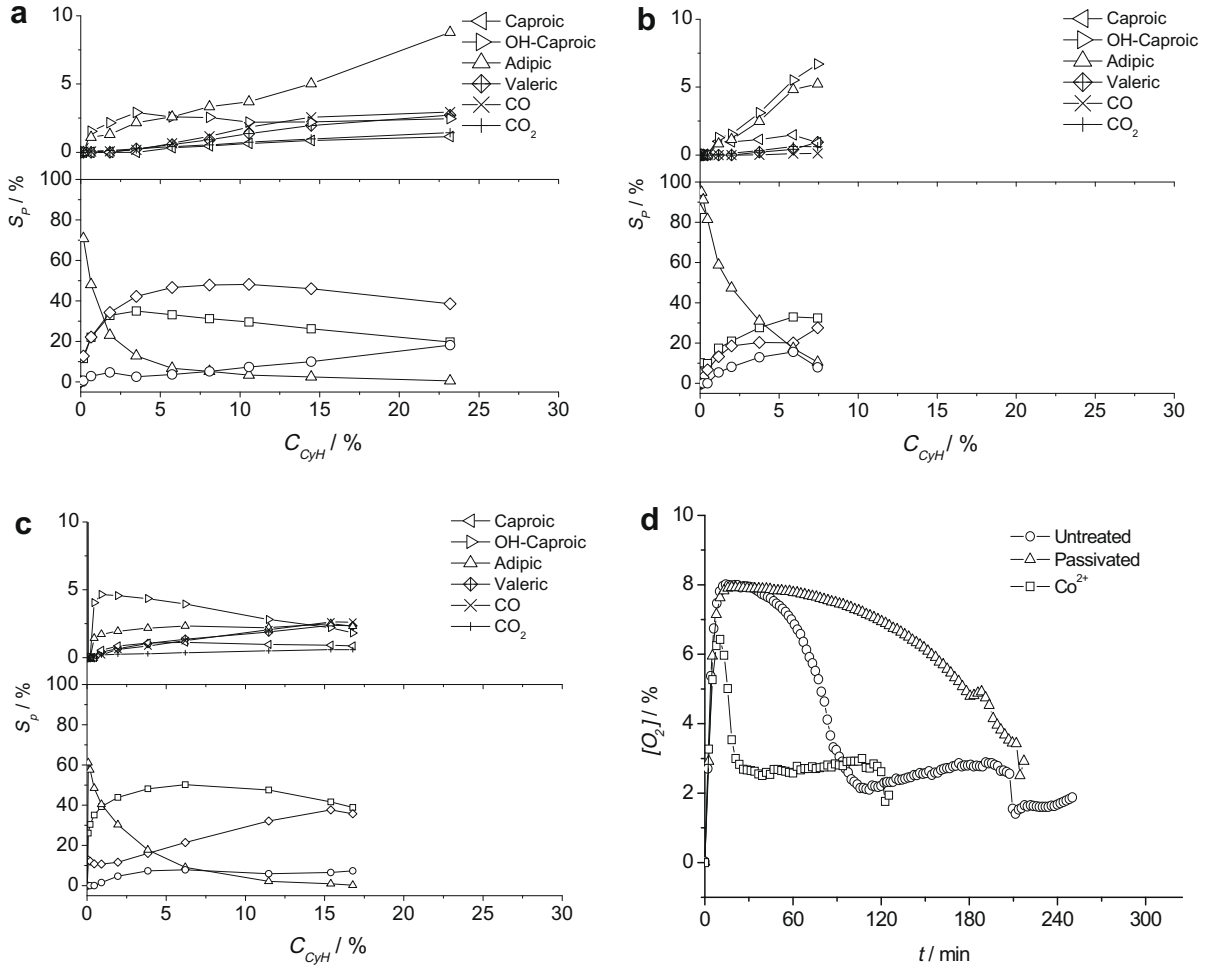

Fig. 4. Product selectivities versus conversion during cyclohexane autoxidation at 150 °C and 1.2–1.5 MPa pressure; untreated reactor (a), passivated reactor (b), Co^{2+} (c), and outlet oxygen concentration (d). $S_{Cy=O}$ (◇), S_{CyOH} (□), S_{CyOOH} (Δ), and S_{C_6} (○).

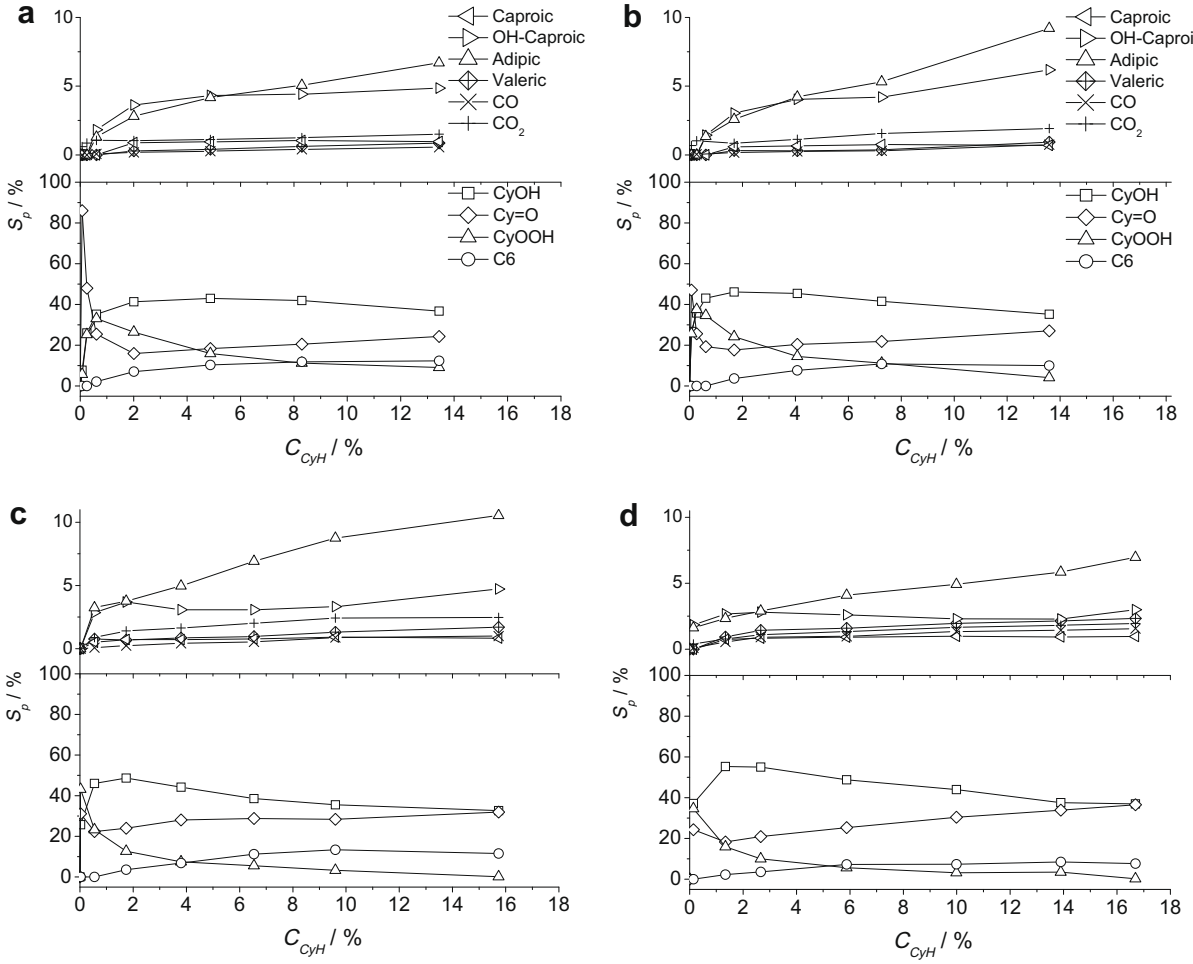

Fig. 5. Product selectivities versus conversion during gold-catalyzed cyclohexane oxidation at 150 °C and 1.2–1.5 MPa pressure; Au/Al_2O_3 (a), Au/TiO_2 (b), Au/SBA-15 (c), and Au/SBA-15 + 1.5 ppm Co^{2+} (d).

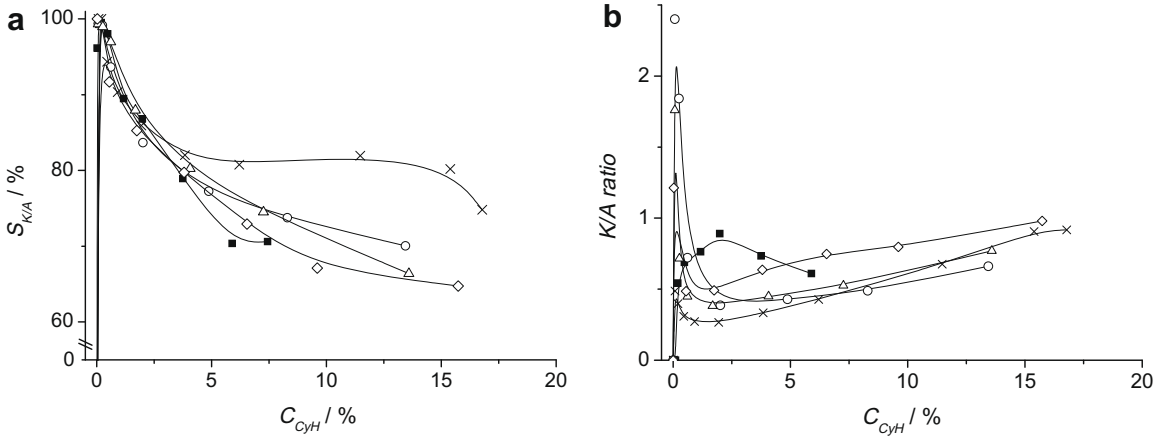

Fig. 6. K/A selectivity (a) and ratio (b) development with increasing cyclohexane conversion at 150 °C and 1.2–1.5 MPa. Autoxidation (■), Co^{2+} (×), Au/Al_2O_3 (○), Au/TiO_2 (Δ), and Au/SBA-15 (◇).

adding 1.5 ppm Co^{2+} to the Au/SBA-15-catalyzed oxidation reaction is illustrated in Fig. 7. When combining a gold-based catalyst with Co^{2+}, both the $S_{K/A}$ and the K/A-ratio became affected. Whereas the selectivity at 4% conversion is improved by 5% in the presence of cobalt, the K/A-ratio decreased significantly from 0.64 to 0.43 in the case of Au/SBA-15 combined with Co^{2+}. In the case of Au/TiO_2 this effect was less apparent but unambiguously present.

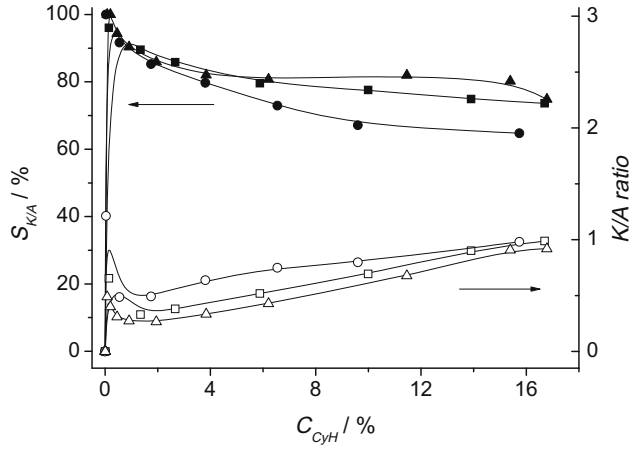

Fig. 7. Influence of cobalt and Au on the $S_{K/A}$ (solid symbols) and K/A-ratio (open symbols) evolution with cyclohexane conversion at 150 °C and 1.2–1.5 MPa. Co^{2+} (▲), Au/SBA-15 (●), and Au/SBA-15 + Co^{2+} (■). 1.5 ppm Co^{2+} was used.

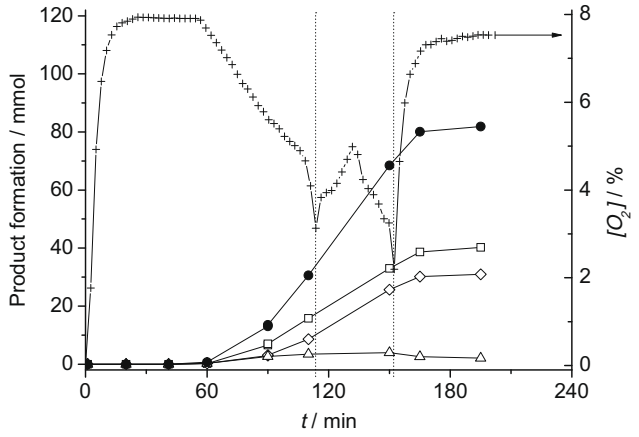

Fig. 8. Cyclohexane oxidation over Au/SBA-15 at 150 °C and 1.0–2.0 MPa in the presence of hydroquinone. CyH conversion (●), formation of Cy=O (◇), CyOH (□) and CyOOH (Δ), and outlet O_2 concentration (+). HQ was added at t = 110 and 150 min.

3.3. Radical inhibition experiments

In order to find additional proof for the hypothesis that the gold-catalyzed oxidation reaction in fact follows a radical-chain mechanism, the free-radical scavenger hydroquinone (HQ) was added to the proceeding oxidation reaction. Hydroquinone can react according to Scheme 2 scavenging oxygen-centered radicals present, thus terminating the radical-chain [33]. The effect of HQ addition on the product formation and O_2 consumption is presented in Fig. 8. At 110 min on stream a small amount of HQ, dissolved in CyH, was added to the reactor and the outlet O_2 concentration increased rapidly from 3.1% to 5.0% decreasing to 3% thereafter. At 150 min on stream when a conversion of 3.5% was reached, a larger amount of HQ (0.5 g dissolved in a 1:1 CyH:acetone mixture) was added and the outlet oxygen concentration increased sharply to 7.5%, almost equal to the inlet concentration. Also the amount of products in the liquid phase remained constant between 165 and 195 min on stream. It is evident that the cyclohexane conversion was completely inhibited after the addition of sufficient HQ to scavenge all free-radicals. The strong yellow color of the liquid-phase samples after HQ addition indicated the formation of benzoquinone, confirming the reaction as described in Scheme 2. A second experiment beheld the addition of HQ initially to the reactor. After 180 min on stream a CyH conversion of 0.015 mol% was reached. Both experiments together proof that the presence of free-radicals is required for both the initiation and propagation phases of the oxidation reaction.

4. Discussion

4.1. Discrepancies with the literature results

In this paper we have compared the performances of gold-based catalysts with those of the classical dissolved cobalt salt and the autoxidation process in the selective oxidation of cyclohexane. Based on TEM analysis we concluded that the Au-based catalysts under study exhibited a similar particle size distribution as the catalyst materials employed for cyclohexane oxidation as reported in the open literature [21–23,25]. Moreover, the applied method of gold deposition is the most widely used procedure and has been proven to yield stable catalyst materials with a small average particle diameter [18,41] which are highly active in a wide variety of oxidation reactions, e.g., propene epoxidation [29,42–44] and partial oxidation of methanol [45]. Based on this we reason that the catalytic performance of these catalyst materials in cyclohexane oxidation is expected to be at least comparable to what is reported in the literature. By performing catalytic test reactions, it was observed that the Au-based catalysts are fairly slow in the conversion of cyclohexane, even slower than the unpassivated stainless steel reactor and the reaction exhibits an initiation period. All the main by-products that were found in the gold-catalyzed oxidation process are known to form in a typical cyclohexane autoxidation reaction [8,13]. Moreover, the gold-based catalysts were found to be less selective at increasing conversion as compared to the commercial alternatives and only show an improvement of the K/A-ratio as compared to using a Co^{2+} initiator. When conducting the oxidation experiments in the presence of a radical scavenger the conversion rate became nil.

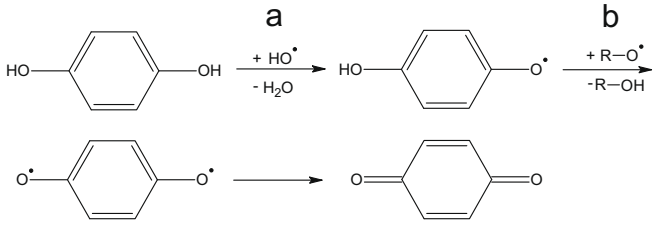

Scheme 2. Mechanism of free-radical scavenging by hydroquinone. HQ reacting with a hydroxy (a) or an alkoxy radical and (b) forming benzoquinone.

By performing a thorough product analysis of the cyclohexane oxidation reaction under industrially relevant conditions it was found that gold-based catalysts do not establish high K/A selectivities (>90%) at high conversions (>10%) as was reported in the open literature [19–25]. Although the gold-based catalysts clearly play a role in directing the oxidation mechanism, it is obvious that the reaction proceeds through a radical-chain mechanism. This is in full agreement with the results published by Xu et al. showing that, at 70 °C, the oxidation reaction over supported Au, Pd, and Pt catalysts would only proceed when *t*-butyl hydroperoxide was initially added as radical initiator [28]. A radical-chain mechanism directly explains the slow initiation of the oxidation reaction by the gold-based catalysts. Since initiation proceeds through a Haber-Weis cycle, the initiation rate strongly depends on the redox potential of the metal. In this regard, gold is not likely to be an efficient initiator. Also, it was already reported earlier that gold catalysts are inefficient in promoting hydrocarbon oxidation by oxygen due to the lack of coordination of hydrocarbons with Lewis acid sites [41]. Our findings in cyclohexane oxidation by Au-based catalysts are completely in agreement with above-mentioned

theories. The reason for this strong deviation from the literature results can be attributed to the complex but required product analysis procedure as was described in the experimental section. In what follows we will elaborate on these encountered complications.

(1) The experiments on gold-based catalysts as described in the literature are performed in a closed batch reactor, which is cooled down and depressurized before collecting the product mixture for analysis. When the reaction mixture is cooled to room temperature before extracting the liquid-phase sample, solubility of various polar molecules (e.g., formic acid, hydroxy-caproic acid, and adipic acid) in cyclohexane decreases dramatically. This complicates the product analysis in that respect that they adsorb on the heterogeneous catalyst and the reactor interior, and care has to be taken to ensure that they are analyzed. Even the addition of a solvent after reaction and stirring for 30 min are not sufficient to extract all organics adsorbed on the catalyst. Therefore it is necessary to extract the liquid samples when they are still at reaction temperature and dissolve them in a suitable solvent before analysis.
(2) The nature of the by-products causes complications during analysis as well. The main important side product, CyOOH, is thermally unstable and readily decomposes upon GC injection giving approximately equal amounts of cyclohexanone and cyclohexanol [46]. To overcome this problem low temperature injection, reduction with triphenyl phosphine, and derivatization methods are reported [13,21,46,47]. Furthermore, it is known that mono- and poly-functionalized organic acids can strongly adsorb on the GC column during analysis, causing broad and overlapping peaks, or in the worst case, do not elute from the column at all. In very few cases the volatility of organic acids is sufficient to allow a direct GC analysis [48]. The high boiling point of, for example, adipic acid (610 K) will cause the molecules to (partially) crystallize already in the GC injector. At conversions >5%, adipic acid itself accounts for 5–10% of all products and might not reach the detector. All the above illustrates the urge of derivatizing –OH-containing compounds into trimethylsilyl or alkyl esters prior to analysis. This makes the molecules less polar, more volatile, and thermally stable and therefore enables quantification by GC [47,49].
(3) Significant amounts of gas-phase products (2–4% of the reacting CyH) are formed, which will be lost when depressurizing the reactor. Thus, in order to obtain a complete carbon balance, the gas phase should be monitored on-line as well.
(4) Due to the continuous gas feed and sample extraction there will be a significant evaporation loss of cyclohexane during reaction. A complete mass balance therefore is not possible to obtain directly from GC analysis and the total conversion thus has to be calculated from the formation of products. In other words, the use of a suitable internal standard in the reactor is inevitable.

Not considering the above-mentioned phenomena will unfortunately lead to an unnoticed incomplete mass balance, and therefore misleading high selectivities.

4.2. Influence of gold-based catalysts on the oxidation mechanism

We observed that the Au-based catalysts have a clear influence on the radical-chain mechanism and can compete with 1.5 ppm dissolved Co^{2+}, which merely accelerated the initiation, leaving the product distribution typical for gold. In the following section we will discuss some influences of the Au-based catalysts on the oxidation mechanism.

4.2.1. CO versus CO_2 formation

One significant difference in the autoxidation and cobalt-catalyzed reaction is the high S_{CO_2} compared to S_{CO}. CO formation was proposed by Hermans et al. to originate from the slow decomposition of CH_3–$(CH_2)_4$–C·=O under oxygen starvation causing the formation of monofunctionalized acids namely valeric acid and butyric acid [13]. Indeed the formation of CO coincides with the appearance of valeric acid and butyric acid. CO_2 formation was in the same publication ascribed to the unimolecular elimination of CO_2 from an acyloxy radical (·OC(=O)–$(CH_2)_4$C(=O)OH) leading, via propagation reactions similar to hydroxy-caproic acid propagation, to the formation of glutaric acid. The origin of the acyloxy radical was found in propagation reactions of hydroxy-caproic acid. Indeed, when no Au-based catalyst is present in the reactor an induction period for both CO_2 and glutaric acid is observed, consistent with the mechanism presented by Hermans et al. However, when there is a gold-based catalyst present, a significant increase in CO_2 formation is observed and in addition CO_2 formation starts at an earlier stage in the reaction even before glutaric acid is observed. This can be clarified by the selective oxidation of CO to CO_2 by the gold-based catalysts. These catalyst materials are known to be very active for this particular reaction at the applied temperature and again confirm that the catalyst materials under study are indeed active catalysts [50,51].

4.2.2. Hydroxy-caproic acid and adipic acid formation

Here we address the observed differences between the formation of the two main oxidation by-products, hydroxy-caproic acid and adipic acid, in a cobalt- and gold-catalyzed cyclohexane oxidation. Hermans et al. identified hydroxy-caproic acid as the first by-product in the cyclohexane autoxidation from which other by-products are formed. Adipic acid formation starts with the αH abstraction from the alcohol functionality of hydroxy-caproic acid by CyOO·, leaving an α-hydroxy-alkyl radical. This reaction was calculated to face a high energy barrier. Therefore, the radical conversion of hydroxy-carpoic acid to adipic acid is slow and occurs on the timescale of hours [13]. This explains the observed convex shape in the evolution of hydroxy-carpoic acid as a function of the total amount of by-products (Fig. 9a). Adipic acid formation is initially lower, but evolves more or less linearly. This means that for the cobalt-catalyzed reaction, hydroxy-caproic acid is initially built up and subsequently converted slowly into other oxidation products, mainly adipic acid. This is in full agreement with and explains the observed fast initial drop in $S_{K/A}$ and subsequent stabilization at ~80% between 5% and 10% conversion (Fig. 6).

In the case of the gold-catalyzed reaction (Fig. 10b), hydroxy-caproic and adipic acids are observed initially in almost equal amounts. This indicates that adipic acid here is rather a primary by-product than a secondary product [52]. Since both by-products are initially observed in equal amounts, both formation rates must be of similar magnitude. This implies that the dominant by-product formation mechanism differs when a heterogeneous catalyst is added. In the case of the Au-catalyzed oxidation reaction up to ~5% conversion, a linear decrease in $S_{K/A}$ is observed (Fig. 6). This can be directly ascribed to the observed enhanced hydroxy-caproic acid and adipic acid formation.

4.2.3. Combining Au and Co^{2+}

As described in the results section, a combination of cobalt and gold as catalyst led to a performance being more or less the average of the fast cobalt and the slow gold catalysts (Fig. 4). However, there are two remarkable effects of adding a gold catalyst. First of all, it is observed that the reaction using a gold-based catalyst as

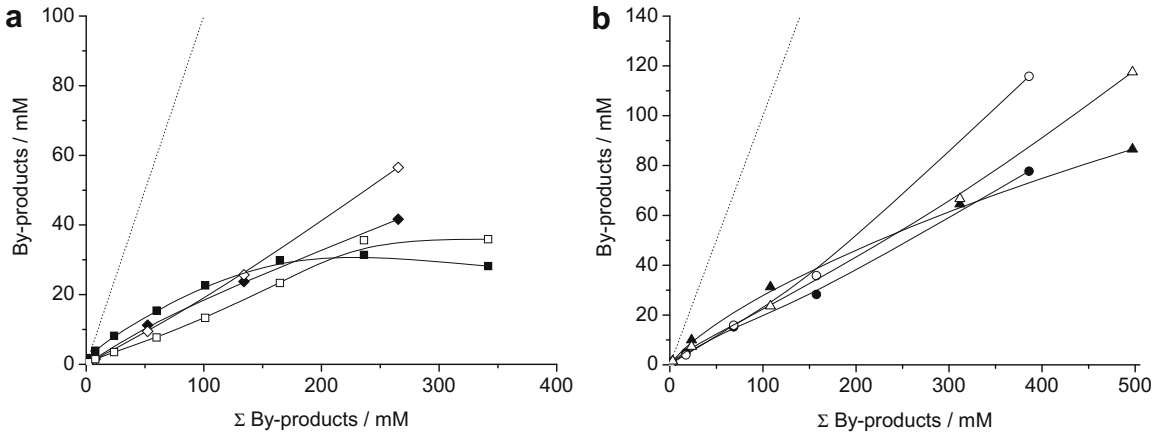

Fig. 9. Evolution of by-products, hydroxy-caproic acid (solid symbols) and adipic acid (open symbols), as the function of the sum of all by-products formed in CyH oxidation at 150 °C and 1.2–1.5 MPa over Co^{2+} (□) and Co^{2+} + TiO_2 (◇) (a), Au/TiO_2 (○), and Au/TiO_2 + Co^{2+} (△) (b).

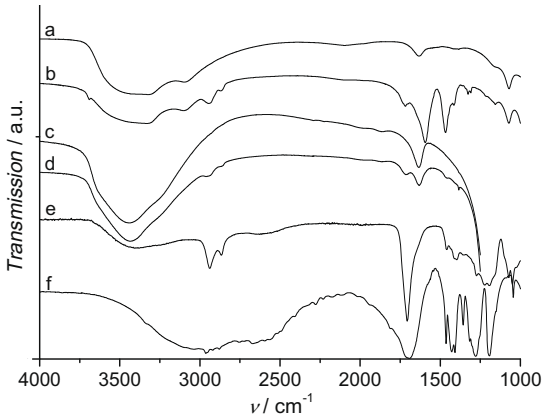

Fig. 10. FT-IR spectra of Au/Al_2O_3 fresh (a) and spent (b) and Au/SBA-15 fresh (c) and spent (d), hydroxy-caproic acid (e) and adipic acid (f).

well as 1.5 ppm Co^{2+} exhibits slower initiation compared to Co^{2+} on its own. Here the gold-based catalysts seemed to function as an inhibitor rather than a catalyst. Secondly, it was observed that when both catalysts were combined, although the influence of cobalt is obvious, the oxidation reaction more or less mimicked the product selectivity characteristics of the gold-catalyzed reaction. This is illustrated by the hydroxy-caproic evolution and adipic acid evolution shown in Fig. 9b which are significantly enhanced in the presence of a gold-based catalyst. Both observations suggest a somehow strong interaction between the Au-based catalyst and the propagating radical intermediates, products, or by-products. Strong adsorption of species on the catalyst surface enables competition between the gold particles and the faster Co^{2+}-mediated cage reactions. Additionally, adsorption of hydroxy-caproic acid on the catalyst surface might facilitate the αH-abstraction from hydroxy-caproic acid by CyOO·, by stabilizing the α-hydroxy-alkyl radical product, thus enhancing the adipic acid formation rate. As described gold-based catalysts will be able to dictate the product and by-product formation. This is in agreement with the observed relative low initial CyOOH selectivity favoring product formation.

The strong sorption of reaction intermediates was confirmed by introducing 0.75 g TiO_2 in the cobalt-catalyzed reaction. The evolution of hydroxy-caproic and adipic acid concentration followed the trend as is observed for the gold-catalyzed reaction (Fig. 9a). This proofs that adsorption of intermediate oxygenate species strongly influenced the by-product formation. Coloring of the white TiO_2 to a brown/yellow color after reaction (and even after dissolution of the reactor content in excess acetone) also indicates strong adsorption of organics. FT-IR spectra recorded of the spent catalysts revealed additional bands around 2850–2950, 1710, and 1460 cm^{-1} resembling the spectra of hydroxy-caproic acid and adipic acid (Fig. 10) confirming the posed hypothesis.

5. Conclusions

The catalytic oxidation of cyclohexane with molecular oxygen over gold-based catalysts was compared with the classic autoxidation and cobalt-catalyzed processes. The different gold-based catalysts under study did not show significant deviations in catalytic performance. It was found that the gold-based catalysts are not efficient in initiating the reaction, which resulted in a long induction period. The products and by-products formed during the gold-catalyzed oxidation of cyclohexane are typical for those found in the autoxidation and cobalt-catalyzed oxidation processes, although a higher product yield could be obtained with both processes. The K/A-ratios over gold-based catalysts are slightly higher compared to those obtained with cobalt, however, lower compared to the autoxidation and not near the 1.5 obtained easily by catalytic CyOOH decomposition. In fact, the gold-based catalysts performed poorly compared to the autoxidation and the cobalt-catalyzed cyclohexane oxidation in terms of selectivity, K/A-ratio, and initiation rate. The low selectivity of the gold-based catalysts was largely caused by the enhanced formation of hydroxy-caproic and adipic acids. Addition of a free-radical scavenger to the reaction slurry initially and at 3.5% conversion completely inhibited the oxidation reaction. Summarizing, we have found the experimental evidence that cyclohexane oxidation in the presence of gold-based catalysts is not a catalytic process, but proceeds through a radical-chain mechanism well known from autoxidation.

Acknowledgments

This research was performed with the financial support from the ACTS/ASPECT program. Rudy Parton and Corinne Daguenet (DSM Research, Geleen, the Netherlands) are kindly thanked for many fruitful discussions. Ad Mens and Vincent Koot (Utrecht University) are acknowledged for their assistance in designing and building the experimental setup. Cor van der Spek (Utrecht University) is thanked for the TEM analysis.

References

[1] E. Bartholomé, Cyclohexanol and cyclohexanone, in: neubearb. und erw. Aufl. (Eds.), Ullmanns Encyklopädie der Technischen Chemie, vol. 4, Weinheim, 1972.
[2] U. Schuchardt, D. Cardoso, R. Sercheli, R. Pereira, R.S. de Cruz, M.C. Guerreiro, D. Mandelli, E.V. Spinace, E.L. Fires, Appl. Catal. A: General 211 (2001) 1.
[3] R.A. Sheldon, J.K. Kochi, Metal-Catalyzed Oxidations of Organic Compounds, Academic Press, New York, 1981.
[4] J.R. Chen, Process Saf. Prog. 23 (2004) 72.
[5] U.F. Kragten, H.A.C. Baur, European Patent EP 0659726 B1, 1994, DSM N.V.
[6] A. Ramanathan, M.S. Hamdy, R. Parton, T. Maschmeyer, J.C. Jansen, U. Hanefeld, Appl. Catal. A: General 355 (2009) 78.
[7] H.A.C. Baur, U.F. Kragten, EP0367326 A1, 1990, DSM N.V.
[8] C.A. Tolman, J.D. Druliner, M.J. Nappa, N. Herron, Alkane oxidation studies in Du Pont's central research department, in: C.L. Hil (Ed.), Activation and Functionalization of Alkanes, first ed., Wiley-Interscience, New York, 1989, p. 316.
[9] R.P. Houghton, C.R. Rice, Polyhedron 15 (1996) 1893.
[10] D.L. Vanoppen, D.E. Devos, M.J. Genet, P.G. Rouxhet, P.A. Jacobs, Angew. Chem. Int. Ed. 34 (1995) 560.
[11] L. Vereecken, T.L. Nguyen, I. Hermans, J. Peeters, Chem. Phys. Lett. 393 (2004) 432.
[12] G. Franz, R.A. Sheldon, Oxidation, in: neubearb. und erw. Aufl. (Eds.), Ullmanns Encyklopädie der Technischen Chemie, vol. 4, Weinheim, 1972.
[13] I. Hermans, P. Jacobs, J. Peeters, Chem. Eur. J. 13 (2007) 754.
[14] I. Hermans, P.A. Jacobs, J. Peeters, J. Mol. Catal. A: Chem. 251 (2006) 221.
[15] I. Hermans, T.L. Nguyen, P.A. Jacobs, J. Peeters, ChemPhysChem 6 (2005) 637.
[16] C. Della Pina, E. Falletta, L. Prati, M. Rossi, Chem. Soc. Rev. 37 (2008) 2077.
[17] A.S.K. Hashmi, G.J. Hutchings, Angew. Chem. Int. Ed. 45 (2006) 7896.
[18] G.C. Bond, D.T. Thompson, Catal. Rev.-Sci. Eng. 41 (1999) 319.
[19] G.M. Lü, R. Zhao, G. Qian, Y.X. Qi, X.L. Wang, J.S. Suo, Catal. Lett. 97 (2004) 115.
[20] R. Zhao, D. Ji, G.M. Lü, G. Qian, L. Yan, X.L. Wang, J.S. Suo, Chem. Commun. (2004) 904.
[21] L.X. Xu, C.H. He, M.Q. Zhu, S. Fang, Catal. Lett. 114 (2007) 202.
[22] L.X. Xu, C.H. He, M.Q. Zhu, K.J. Wu, Y.L. Lai, Catal. Commun. 9 (2008) 816.
[23] L.X. Xu, C.H. He, M.Q. Zhu, K.J. Wu, Y.L. Lai, Catal. Lett. 118 (2007) 248.
[24] G.M. Lü, D. Ji, G. Qian, Y.X. Qi, X.L. Wang, J.S. Suo, Appl. Catal. A: General 280 (2005) 175.
[25] K.K. Zhu, J.C. Hu, R. Richards, Catal. Lett. 100 (2005) 195.
[26] L. Li, C. Jin, X.C. Wang, W.J. Ji, Y. Pan, T. van der Knaap, R. van der Stoel, C.T. Au, Catal. Lett. 129 (2009) 303.
[27] G.J. Hutchings, S. Carrettin, P. Landon, J.K. Edwards, D. Enache, D.W. Knight, Y.J. Xu, A.F. Carley, Top. Catal. 38 (2006) 223.
[28] Y.J. Xu, P. Landon, D. Enache, A. Carley, M. Roberts, G. Hutchings, Catal. Lett. 101 (2005) 175.
[29] T.A. Nijhuis, B.J. Huizinga, M. Makkee, J.A. Moulijn, Ind. Eng. Chem. Res. 38 (1999) 884.
[30] D.Y. Zhao, Q.S. Huo, J.L. Feng, B.F. Chmelka, G.D. Stucky, J. Am. Chem. Soc. 120 (1998) 6024.
[31] J.R. Chenn, Process Saf. Prog. 23 (2004) 72.
[32] J.R. Chenn, K. Liu, AIChE J. 49 (2003) 2427.
[33] A.P. Pokutsa, A.B. Zaborovskii, R.B. Sheparovich, V.I. Kopylets, D.S. Maksim-Lutsik, Kinet. Catal. 44 (2003) 121.
[34] R. Raja, G. Sankar, J.M. Thomas, J. Am. Chem. Soc. 121 (1999) 11962.
[35] M.C. Daniel, D. Astruc, Chem. Rev. 104 (2004) 293.
[36] X-ray powder diffraction patterns where compared with entries from the PDF JCP2 database.
[37] By passivation, exogenous metal ions are extracted from the stainless steel reactor interior surface. Stainless steel F316 contains Cr (16–18%), Ni (10–14%) and Mo (2–3%) ions which can leach into the reaction mixture under the severe reaction conditions and participate in the catalysis. Especially Cr-ions are known to be active in cyclohexane oxidation and very susceptible to leaching.
[38] By reaction with PPh_3 hydroperoxo-groups will reduce to form an alcohol functionality. In some cases an increase in the 6-hydroxycaproic acid concentration was observed after such treatment of the sample, indicating the presence of 6-hydroperoxo-caproic acid.
[39] E. Breynaert, I. Hermans, B. Lambie, G. Maes, J. Peeters, A. Maes, P. Jacobs, Angew. Chem. Int. Ed. 45 (2006) 7584.
[40] I. Hermans, P.A. Jacobs, J. Peeters, Chem. Eur. J. 12 (2006) 4229.
[41] A. Corma, H. Garcia, Chem. Soc. Rev. 37 (2008) 2096.
[42] T.A. Nijhuis, T. Visser, B.M. Weckhuysen, J. Phys. Chem. B 109 (2005) 19309.
[43] T.A. Nijhuis, T. Visser, B.M. Weckhuysen, Angew. Chem. Int. Ed. 44 (2005) 1115.
[44] E. Sacaliuc, A.M. Beale, B.M. Weckhuysen, T.A. Nijhuis, J. Catal. 248 (2007) 235.
[45] B.P.C. Hereijgers, B.M. Weckhuysen, ChemSusChem 2 (2009) 743.
[46] G.B. Shulpin, D. Attanasio, L. Suber, J. Catal. 142 (1993) 147.
[47] S.B. Turnipseed, A.J. Allentoff, J.A. Thompson, Anal. Biochem. 213 (1993) 218.
[48] P. Englmaier, J. Chromatogr. 194 (1980) 33.
[49] T. Niwa, J. Chromatogr. 379 (1986) 313.
[50] M. Haruta, S. Tsubota, T. Kobayashi, H. Kageyama, M.J. Genet, B. Delmon, J. Catal. 144 (1993) 175.
[51] M. Haruta, N. Yamada, T. Kobayashi, S. Iijima, J. Catal. 115 (1989) 301.
[52] I. Hermans, J. Van Deun, K. Houthoofd, J. Peeters, P.A. Jacobs, J. Catal. 251 (2007) 204.